Article

Thermotropic Uniaxial and Biaxial Nematic and Smectic Phases in Bent-Core Mesogens

Veena Prasad, Shin-Woong Kang, K. A. Suresh, Leela Joshi, Qingbing Wang, and Satyendra Kumar

J. Am. Chem. Soc., **2005**, 127 (49), 17224-17227• DOI: 10.1021/ja052769n • Publication Date (Web): 15 November 2005

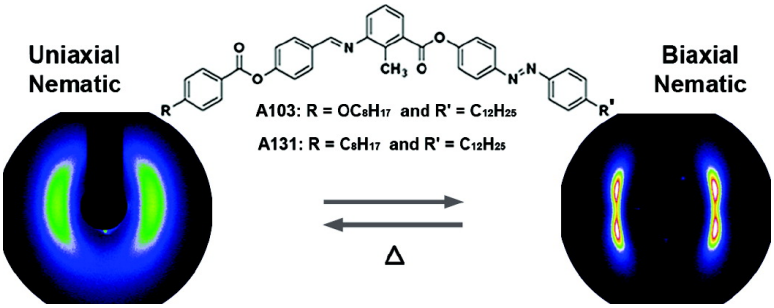

More About This Article

Additional resources and features associated with this article are available within the HTML version:

- Supporting Information
- Links to the 12 articles that cite this article, as of the time of this article download
- Access to high resolution figures
- Links to articles and content related to this article
- Copyright permission to reproduce figures and/or text from this article

View the Full Text HTML

J|A|C|S
ARTICLES
Published on Web 11/15/2005

Thermotropic Uniaxial and Biaxial Nematic and Smectic Phases in Bent-Core Mesogens

Veena Prasad,[†] Shin-Woong Kang,*[,‡] K. A. Suresh,[§] Leela Joshi,[‡] Qingbing Wang,[‡] and Satyendra Kumar[‡]

Contribution from the Center for Liquid Crystal Research, P.O. Box 1329, Jalahalli, Bangalore 560 013, India, Department of Physics, Kent State University, Kent, Ohio 44242, and Raman Research Institute, Sadashivanagar, Bangalore 560 080, India

Received April 28, 2005; Revised Manuscript Received September 23, 2005; E-mail: skang1@kent.edu

Abstract: Two azo substituted achiral bent-core mesogens have been synthesized. Optical polarizing microscopy and synchrotron X-ray scattering studies of both compounds reveal the existence of the thermotropic *uniaxial* and *biaxial* nematic and three smectic phases at different temperatures in these single component small molecule systems. The transition from the uniaxial to biaxial nematic phase is confirmed to be second order. The transitions from the biaxial nematic to the underlying smectic phase and between the smectic phases have barely discernible heat capacity signatures and thus are also second order.

Introduction

Since Freiser's prediction[1] of the existence of the biaxial nematic (N_b) phase nearly 32 years ago, this topic has attracted much attention due to its interesting static and dynamic properties and potential device applications with the possibility of much faster switching.[2] In the uniaxial nematic (N_u) phase, the molecular axes are oriented along the director **n**, whereas, in the N_b phase, there exists additional orientational order along a second axis, or secondary director **m**, that is perpendicular to **n**. Thus, in the N_b phase, the physical properties in the plane perpendicular to **n** are anisotropic. It should be possible to control the orientation of **m** with an applied field, leading to potentially 100 times faster new types of electro-optical devices which hold the potential to revolutionize the display industry.

Several previous claims[3,4] of the discovery of the N_b phase in low molecular-mass liquid crystals (LCs) have remained unsubstantiated.[5,6] Consequently, the N_b phase remained elusive and much sought[2,5−7] after. However, recent X-ray studies marked the discovery[8] of the N_b phase in bent-core mesogens, later confirmed by NMR studies.[9] It was predicted that the N_b phase could form in single-component systems with optimized molecular shape-biaxiality.[10] Theoretical investigations[11−13] and simulations[14] have yielded phase diagrams with two uniaxial phases and one biaxial nematic phase and predicted the uniaxial to biaxial nematic phase transitions to be second order. The transition from the N_b phase to the smectic-C (SmC) phase has been compared with the N_b to smectic-A transition and is also expected[15] to be second order. These interesting predictions and the recent discovery of the N_b phase[8] have prompted researchers to pursue synthesis of more suitable bent-core compounds.[16,17]

Here, we report the first observation of the existence of, both, the N_u and N_b phases in two bent-core compounds with the help of optical polarizing microscopy (POM) and synchrotron X-ray diffraction (XRD). These materials provide us with an opportunity to study the nature of the transitions between the Isotropic (I), N_u, N_b, and three underlying smectic phases.

Results and Discussion

Molecular structures, phase sequences, and transition temperatures for the two compounds are shown in Figure 1. Synthesis of these compounds was achieved using a procedure similar to the one previously reported[16,17] by us. The experimental details on synthesis are described in the Supporting

[†] Center for Liquid Crystal Research.
[‡] Department of Physics, Kent State University.
[§] Raman Research Institute.

(1) Freiser, M. J. *Phys. Rev. Lett*. **1970**, *24*, 1041.
(2) Luckhurst, G. R. *Thin Solid Films* **2001**, *393*, 40.
(3) Chandrasekhar, S.; Nair, G.; Rao, D. S. S.; Prasad, S. K.; Praefcke, K.; Singer, D. *Mol. Cryst. Liq. Cryst.* **1996**, *288*, 7.
(4) Malthele, J.; Leibert, L.; Levelut, A. M.; Galerne, y. *C. R. Acad. Sci. Paris* **1986**, *303*, 1073.
(5) Shenouda, I. G.; Shi, Y.; Neubert, M. *Mol. Cryst. Liq. Cryst.* **1994**, *257*, 209.
(6) Hughes, J.; Kothe, G.; Luckhurst, G. R.; Malthete, J.; Neubert, M. E.; Shenouda, I.; Timimi, B. A.; Tittelbach, M. *J. Chem. Phys.* **1997**, *107*, 9252.
(7) Praefcke, K.; Blunk, D.; Singer, D.; Goodby, J. W.; Toyne, K. J.; Hird, M.; Styring, P.; Norbert, W. D. J. A. *Mol. Cryst. Liq. Cryst*. **1998**, *323*, 231.
(8) Acharya, B. R.; Primak, A.; Kumar, S. *Phys. Rev. Lett*. **2004**, *92*, 145506-1. Acharya, B. R.; Primak, A.; Dingemans, T. J.; Samulski, E. T.; Kumar, S. *Pramana*, **2003**, *61*, 231. Acharya, B. R.; Primak, A.; Kumar, S. *Liq. Cryst. Today* **2004**, *13*, 1.
(9) Madsen, L. A.; Dingemans, T. J.; Nakata, M.; Samulski, E. T. *Phys. Rev. Lett*. **2004**, *92*, 145505-1.
(10) Praefcke, K.; Kohne, B.; Gundogan, B.; Singer, D.; Demus, D.; Diele, S.; Pelzl, G.; Bakawsky, U. *Mol. Cryst. Liq. Cryst*. **1991**, *198*, 393.
(11) Alben, R. *J. Chem. Phys.* **1973**, *59*, 4299.
(12) Allender, D. W.; Lee, M. A.; Hafiz, N. *Mol. Cryst. Liq. Cryst*. **1985**, *124*, 45.
(13) Vissenberg, M. C. J. M.; Stallinga, S. *Phys. Rev*. **1997**, *E55*, 4367.
(14) Frenkel, D.; Eppenga, R. *Phys. Rev. Lett.* **1982**, *49*, 1089.
(15) Brand, H. R.; Pleiner, H. *Makromol. Chem., Rapid Commun.* **1991**, *12*, 539. Grienstein, G.; Toner, J. *Phys. Rev. Lett.* **1981**, *51*, 2386.
(16) Prasad, V.; Kang, S.-W.; Kumar, S. *J. Mater. Chem.* **2003**, *13*, 1259.
(17) Prasad, V.; Jakli, A. *Liq. Cryst*. **2004**, *31*, 473.

10.1021/ja052769n CCC: $30.25

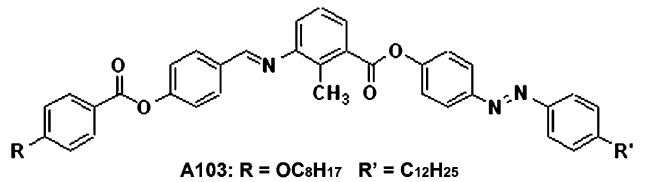

Figure 1. Molecular structures, phases, and transition temperatures for compounds **A103** and **A131**.

Information. Below, we discuss the results obtained for compounds ***A103*** and ***A131***.

Optical cells made with homeotropic and planar boundary conditions on glass substrates were examined under POM as the sample temperature was lowered. The optical textures obtained at different temperatures are shown in Figure 2. As clear from Figure 2c, the biaxial nematic phase exhibited typical Schlieren nematic texture after the transition from the uniaxial nematic phase.

The results of differential scanning calorimetry (DSC), shown in Figure 3, revealed latent heats of melting, 40.8 and 34.5 kJ/mol, and clearing, 0.68 and 0.63 kJ/mol, for **A103** and **A131**, respectively. The N_u to N_b transition of **A131**, very evident in POM and X-ray measurements discussed below, was not discernible in the DSC scans. The N_b to SmC transition and the transitions among lower temperature smectic phases appeared either as a very small peak or a cusp in the DSC theromograph. For **A103**, a small cusp marked the N_u to N_b transition. The absence of measurable latent heat at these transitions indicated that they are essentially second order.

X-ray work was performed at the Midwestern Universities Collaborative Access Team's sector at the Advanced Photon Source of the Argonne National Laboratory. XRD patterns were acquired using a high-resolution image plate detector MAR-345 placed at 1158.9 mm from the sample and $\lambda = 0.7653$ Å.

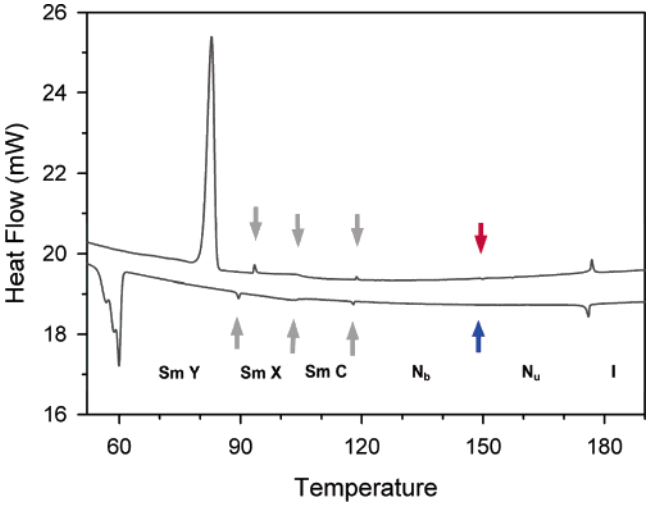

Figure 3. DSC thermograph of **A131**, taken at 5 °C/min, during heating (upper curve) and cooling (lower curve) cycles. Latent heats of 34.5 and 0.63 kJ/mol are measured at the melting and clearing points near 84 and 177 °C, respectively. No signature of the N_u to N_b transition is discernible. A small peak at the N_b to SmC transition is visible near 120 °C.

The 2-D XRD patterns were analyzed using the software package FIT2D written by A. P. Hammersley of the European Synchrotron Radiation Facility.

The samples were aligned by cooling from the I phase in the presence of a magnetic field of ~0.25 T, produced by a pair of CoSm magnets, perpendicular to the X-ray beam. The X-ray diffraction patterns were acquired at various temperatures. At all temperatures, the wide-angle reflections corresponded to an overall lateral dimension of ~5.3 Å of molecules. These *liquidlike* reflections implied the lack of positional order within smectic layers. Small angle peaks in different mesophases are shown on an expanded scale in Figure 4.

Data analysis was carried out to generate integrated intensity vs diffraction angle plots for scans at different temperatures. These were used to determine the temperature dependence of

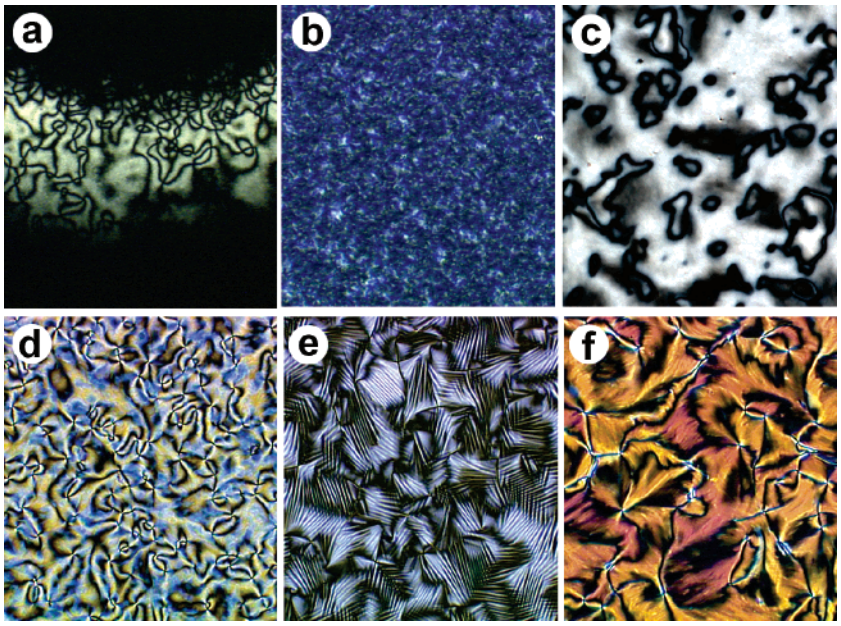

Figure 2. POM textures of **A131**. (a) The isotropic (I) phase transforming in to the N_u phase at 176.5 °C in homeotropic configuration, (b) the N_b phase upon cooling the homeotropically aligned N_u phase to 122 °C, (c) N_b texture with planar boundary condition at 122 °C, (d) Schlieren SmC texture at 112 °C, (e) unidentified SmX phase at 96 °C, and (f) the SmY phase at 84 °C.

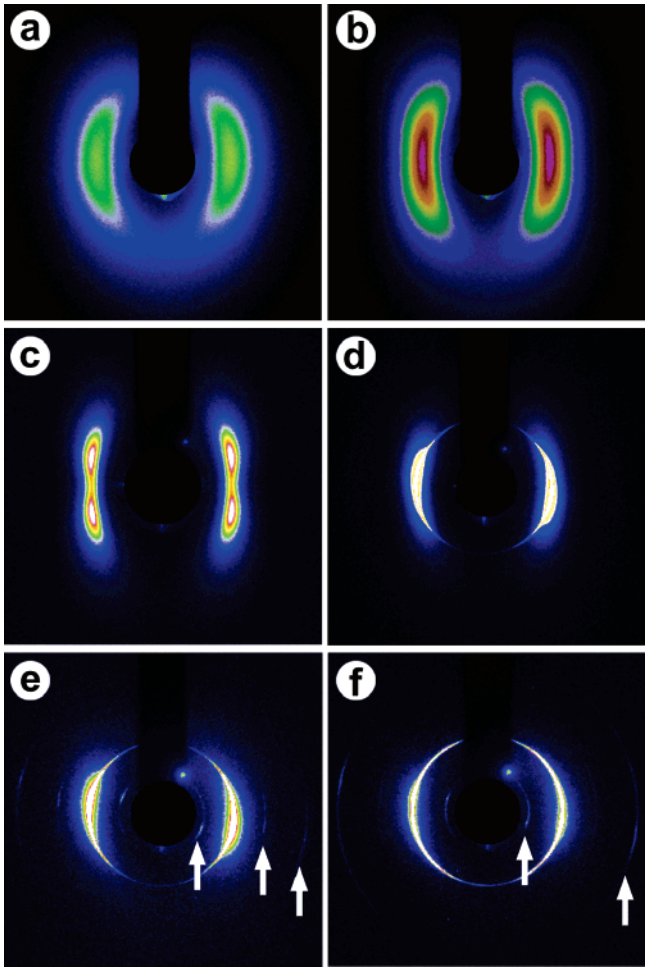

Figure 4. X-ray diffraction patterns in the (a) N_u phase at 176.0 °C, (b) N_u phase at 163.2 °C, (c) N_b phase at 120.7 °C, (d) SmC phase (107.2 °C), (e) SmX phase (94.4 °C), and (f) SmY phase (83.2 °C) of compound **A131**. The arrows mark the additional peaks that appear in SmX and SmY phases.

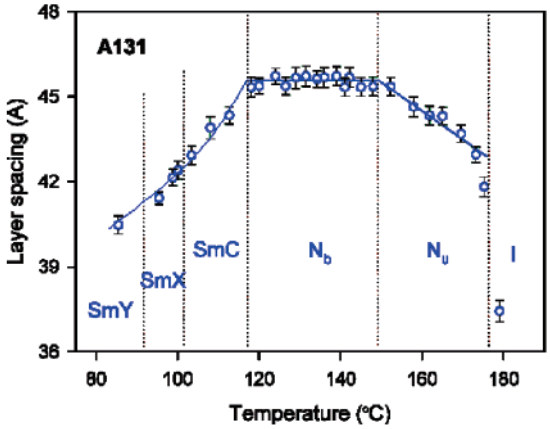

Figure 5. Layer spacing calculated from the position of the Bragg peak as a function of temperature.

the layer spacing, *d*, and full width at half-maximum (fwhm) shown in Figures 5 and 6, respectively.

The distinct POM textures for **A131** confirmed the existence of two nematic and three smectic phases. As the sample was cooled from the I phase, a wave front of nematic texture passed through the field of view [Figure 2a] at the transition to the N_u phase at 176.5 °C, which soon attained homeotropic orientation. In the N_u phase, the X-ray diffraction pattern consisted of two

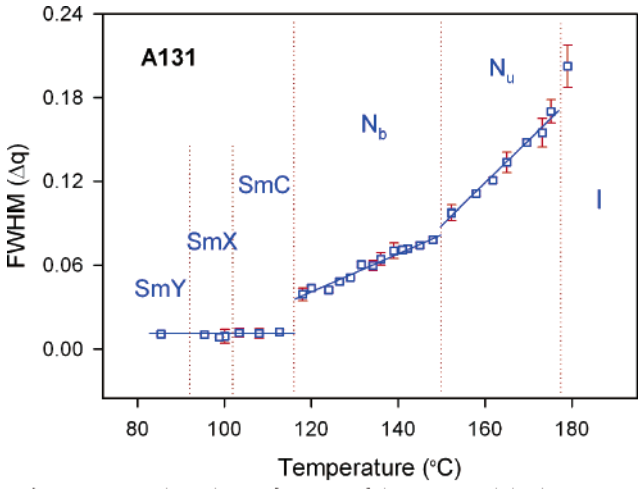

Figure 6. Temperature dependence of *fwhm* of the Bragg peak in the two nematic and smectic phases.

small-angle arcs [Figure 3a] corresponding to the average molecular length of 45.5 Å. At lower temperatures, gray Schlieren texture of the N_b phase developed gradually [Figure 2b] around 149 °C. A nematic like texture also developed in cells prepared with planar boundary conditions, Figure 2c. The two diffraction arcs also developed a slight flatness in the middle, Figure 3b, at the same temperature.

The texture continued to brighten due to an increase in the birefringence related to the biaxial order, i.e., the difference in the indices of refraction ($\Delta n_{xy} = n_x - n_y$) along the two directions in the plane perpendicular to **n**, or the *z*-axis. The brightness of the N_b texture remained much lower than that of typical N_u texture due to much smaller value of Δn_{xy} than the birefringence of the uniaxial phase. The temperature dependence of *d* and the *fwhm*, shown in Figures 5 and 6, showed a marked change at the N_u to N_b transition. The changes in the POM texture, the shape of Bragg reflections, and in the values of *d* and *fwhm* clearly show a phase transition between the two nematic phases. The positional order correlations in the N_u phase varied from $0.75l - 1.5l$ and from $2l$ to $3.3l$ in the N_b phase, l being the length of the **A131** molecule. The nematic arcs fully split into two pairs of reflections in the biaxial phase, giving the characteristic XRD pattern of the biaxial nematic phase[8] of bent-core mesogens, as shown in Figure 4c at 120.7 °C.

At 118 °C, the texture suddenly changed to a Schlieren texture, characteristic of the SmC phase; Figure 2d shows the texture at 112 °C. There were only two X-ray reflections present in the SmC phase: the small angle peak and the large angle peak at 5.3 Å. The small angle XRD pattern changed from two pairs of reflections to clusters of reflections [Figure 4d] lying on a circle, due to granular mosaicity of the SmC phase. The layer spacing in the SmC phase is smaller than the molecular length measured in the nematic phase, due to temperature-dependent molecular tilt. The smectic layer spacing below this transition showed temperature dependence typical of the SmC phase. The positional correlation length (or 1/*fwhm*) was limited by the sample mosaic and made a jump by a factor of more than 4 at this transition. The large angle reflection did not exhibit any significant changes at this transition. One can conclude that these phases retained liquidlike correlations within the smectic layers.

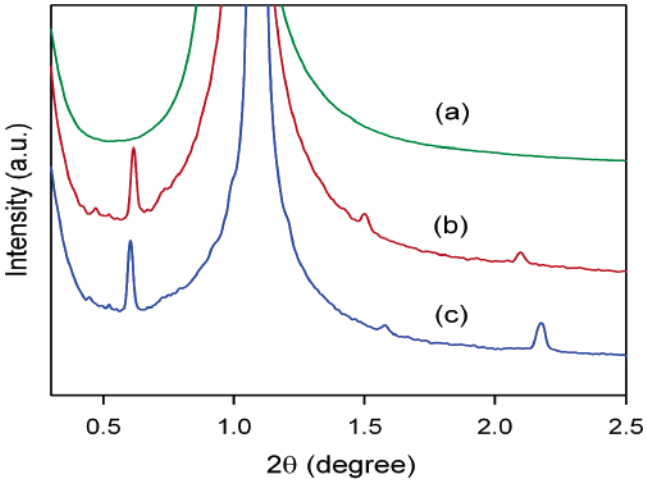

Figure 7. X-ray intensity vs diffraction angle [λ = 0.7653 Å] plots in (a) the SmC phase (107.2 °C), (b) the SmX phase (94.4 °C), and (c) the SmY phase (83.2 °C) of the compound **A131**.

The SmC phase underwent a transition to a yet to be characterized smectic-X (SmX) phase as revealed by the sudden development [Figure 2e] of sets of striations, suggesting a chiral nature. The intensity of the most intense X-ray reflection (at ~43.88 Å) became more evenly distributed. In addition, one peak at 71.2 Å and two weak higher angle reflections appeared at 29.2 and 20.9 Å and are marked by white arrows in Figure 4(e). This change is also evident in the intensity vs diffraction angle plots in Figure 7(a) and (b), generated from the diffraction patterns.

The system exhibited another transition to a second unknown phase, which we refer to as the smectic-Y (SmY) phase. In this phase, the striations of the SmX phase disappeared [Figure 2f]. Its texture appeared to be similar to textures observed in phases with hexatic order. However, we did not see any noticeable sharpening of the large angle reflection to suggest any change in the in-plane order. The intensity of the brightest ring at 41.4 Å [Figure 4f] was significantly redistributed, the intensity of the (third) reflection at 27.8 Å diminished, and the reflections at 71.2 and 20.7 Å, marked with white arrows in Figure 4f, became brighter. These changes can also be gleaned from the graphs in Figure 7b and c.

Essentially similar results were obtained in the corresponding mesophases of **A103**. Except for the difference in transition temperatures, the two compounds appear to be completely isomorphous in their mesogenic properties. Synthesis and a systematic study of the mesomorphic behavior of the homologous series of these compounds are in progress. Further experimental studies are currently being performed to better understand the structure and dynamical behavior of the N_u and N_b phases and the transition between them.

Acknowledgment. One of us (V.P.) is grateful to the Director, Raman Research Institute, where the author is presently visiting, for providing the research facilities used for this work. NMR spectra were recorded at the Sophisticated Instruments Facility, Indian Institute of Science, Bangalore. This work was supported by the National Science Foundation Grant DMR-03-12792. Use of the Advanced Photon Source (APS) was supported by the U.S. Department of Energy, Basic Energy Sciences, Office of Science, under Contract No. W-31-109-Eng- 38. The Midwest Universities Collaborative Access Team (MUCAT) sector at the APS is supported by the U.S. Department of Energy, Basic Energy Sciences, Office of Science, through the Ames Laboratory under Contract No. W-7405-Eng-82.

Supporting Information Available: Experimental details of synthesis. This material is available free of charge via the Internet at http://pubs.acs.org.

JA052769N